Journal of Thermal Analysis and Calorimetry
https://doi.org/10.1007/s10973-019-08449-5

Effect of water flow in a solar still using novel materials

C. Suresh[1] · S. Shanmugan[2]

Received: 21 August 2018 / Accepted: 9 June 2019

Abstract
The effects of novel materials, viz. phase-change material and nanoparticles, and water flowing over a glass cover on the performance of a single-slope single-basin solar still for use in solar thermal applications are presented and discussed. The results obtained with and without PCM and nanoparticles are compared with those for a conventional solar still on summer days. Numerical simulations and experiments were carried out to provide solutions for the temperatures of the flowing water, glass cover, novel materials [i.e., fin with cotton wick (FWCW), fin with jute wick (FWJW), and PCM], and nanoparticle basin liner. The daily production rate of distillate from pure saline water by the solar still was enhanced by using a drip button due to the absorptive capability of FWCW of 70.02%, resulting in daily (24 h) distillate production of 9.429 kg m^{-2} day^{-1}, while the effect of water flowing over the glass cover was 13.37%, being 25% higher than without PCM and nanoparticles, respectively. The enhanced performance of the solar still was investigated using Fourier analysis with harmonics from 6 to −6, revealing good agreement with the observations, validating the theoretical and experimental analysis of the system.

Keywords PCM · Nanoparticles · Fin wick · Drip button · Water flowing over glass cover · Fourier series

List of symbols

b	Breadth of solar still (m)
$C_{Fw} - c_{fw}$	Specific heat of fin wick and flowing water (J kg^{-1} °C^{-1})
H_s	Solar radiation (W m^{-2})
$h_{b+PCM+Nanoparticles}$	Overall bottom heat loss coefficient from basin liner to ambient with improvement due to use of PCM and nanoparticles (W m^{-2} °C^{-1})
h_1	Total heat transfer coefficient from fin wick water surface to glass cover (W m^{-2} °C^{-1})
h_2	Convective and radiative heat transfer coefficient from cooling water flow under glass cover to ambient (W m^{-2} °C^{-1})
h_3	Convective heat transfer coefficient from PCM and nanoparticles by basin liner to water mass (W m^{-2} °C^{-1})
h_4	Convective heat transfer coefficient from glass cover to flowing water (W m^{-2} °C^{-1})
l_w	Thickness of flowing water over glass cover (m)
M_{Fw}	Fin wick mass in basin surface area (kg)
m_{fw}	Mass flow rate of water (kg m^{-2} h^{-1})
$\dot{Q}$	Heat flux of still (W m^{-2})
$\dot{q}_{ew}$	Evaporative heat transfer rate (W m^{-2})
R_1 and R_2	Two constants obtained from saturation vapor data (°C)
T_a	Ambient temperature (°C)
$T_{b+PCM+Nanoparticles}$	Temperature of PCM and nanoparticles in basin surface area (°C)
T_g	Temperature of glass cover (°C)

✉ S. Shanmugan
s.shanmugam1982@gmail.com

C. Suresh
sureshc.struct@gmail.com

[1] Department of Civil Engineering, Vel Tech Multitech Dr. Rangarajan Dr. Sakunthala Engineering College, Avadi, Chennai 600062, Tamil Nadu, India

[2] Research Center of Physics, Koneru Lakshmaiah Education Foundation (KLEF - KLU), Green Fields, Guntur District, Vaddeswaram, Andhra Pradesh 522502, India

Published online: 20 September 2019

T_{fw}	Temperature of flowing water (°C)
T_{Fw}	Temperature of fin wick water surface (°C)
T_s	Surface temperature of sun (°C)

Greek letters

$\alpha_{b+PCM+Nanoparticles}$	Energy absorptivity of PCM and nanoparticles in basin surface area
α_g	Energy absorptivity of glass cover
α_{Fw}	Energy absorptivity of fin wick water mass
α_{fw}	Energy absorptivity of flowing water
η	Energy efficiency of still

Abbreviations

FWCW	Fin with cotton wick
FWJW	Fin with jute wick

Introduction

Water is wasted every day through numerous physical processes but is required by all active cells, as nearly all processes taking place within the body are reliant on water. Solar energy can be used for solar thermal desalination using evaporative cooling to enhance the production of clean water. Numerical modeling of water flowing over the glass cover in a solar still is important to design an optimal still and enhance its performance at given cost. Prakash and Kavatherkar [1] reported the realization of a regenerative still based on a conventional design, achieving a daily yield of around 7.5 L m^{-2}. Singh and Tiwari [2] reported on a passive regenerative solar still, showing good agreement between theoretical and experimental results for the system. An analytical expression for the thermal efficiency of an active regenerative solar still was presented by Singh and Tiwari [3], who found that the overall thermal efficiency of the heat transfer unit and collector was 50%. The yield of concentrator-assisted regenerative solar stills is much higher than that of any other passive/active, regenerative/nonregenerative still designs, and their overall efficiency increases with increase in the flow rate of cold water over the glass cover, as suggested by Sanjay Kumar and Sinha [4]. Prasad et al. [5] reported that regenerative active solar stills show enhanced thermal performance.

Sangeeta Suneja and Tiwari [6] proposed that, for a given flow rate of water over the glass cover, the evaporative heat transfer coefficient decreases with increasing water depth in the basin, whereas the radiative and convective heat transfer coefficients do not change greatly. Zurigat and Abu-Arabi [7] analyzed a double-glass-cover cooling desalination unit, suggesting that the arrangement offered two advantages, viz. lowering the glass temperature and preheating the brine entering the system. Ultimately, the efficiency of the still was increased by more than 25% compared with a conventional single-basin single-glass solar still. Zurigat and Abu-Arabi [8] reported on the performance of a regenerative solar still based on two basin effects (first effect and second effect), achieving a distillate yield 20% higher than that of conventional solar stills. Janarathanan et al. [9] reported on the performance of a tilted wick-type solar still, concluding that the lower temperature of the glass cover, the water flow over the glass cover, and the flow rate of 1.5 m s^{-1} significantly increased the production. Kalidasa Murugavel et al. [10] reviewed the productivity of a single-basin solar still using different materials in the basin, indicating that use of rubber material in the basin improved the absorption, storage, and evaporation effects. Boutenila [11] showed that the initial film thickness, plate inclination, still length, and radiation reaching the flux plate were the factors affecting the performance of such stills. Zeroual et al. [12] investigated a double-slope solar still with two effects, indicating that the productivity was increased by 11.82% by cooling the condenser by flowing water over it (first effect) and 2.94% by shading the north wall from 12:00 to 14:00 h (second effect). The performance of an inverted absorber solar still was reported by Dea et al. [13], who found that its thermal efficiency was thrice that of a normal solar still. Abdul Jabber [14] reported the effect of the tilt angle of a condensing cover on the productivity of a simple solar still in different seasons and at different latitudes. It was found that the tilt angle should be large in winter but small in summer. Sandeep et al. [15] proposed a single-slope single-basin active solar still with an enhanced condensation procedure, reporting a yield improvement of 14.5% compared with the original design. Shanmugan et al. [16] used a thermal model to analyze the energy and exergy of a single-slope single-basin solar still. Rahmani et al. [17] considered the natural circulation in a solar still and established a distillate yield of 3.72 L m^{-2} day^{-1} with efficiency of 45.15%. Ayman et al. [18] amended a basin-type solar still, achieving maximum freshwater production of 2.93 L m^{-2} day^{-1}. A single-slope solar still was integrated into the system to improve the efficiency. Sahota and Tiwari [19] proposed a double-slope solar still using Al_2O_3 nanoparticles in the basin, applying nanofluids with three different concentrations of 0.04%, 0.08%, and 0.12%. The efficiency of the system including Al_2O_3 nanoparticles was 0.12%. The systems with 35 kg and 80 kg of base fluid exhibited efficiency of 12.2% and 8.4%. Shanmugan et al. [20] carried out experimental analysis of a double-slope tribasin solar still, establishing that the use of nanofluids enhanced the performance contributions of the first,

second, and third basins by 35.71%, 35.7%, and 28.5%, respectively. Sellamia et al. [21] explored an enhanced solar still with coatings of different thicknesses of sponge absorber to save more energy while retaining the performance. Liner thicknesses of 0.5 cm, 1.0 cm, and 1.5 cm resulted in harvest improvements of 58%, 23.03%, and 30%, respectively.

Sharshir [22] investigated the effects of flake graphite nanoparticles (FGN), PCM, and film for cooling a solar still. Amendment of the solar still with FGN and PCM resulted in 73.8% higher yield, matching the performance of a conventional still, with total enhancement of 13% for water depths from 2 to 0.5 cm. The heat transfer within the structure was examined over time, as well as the extra energy required to increase the temperature at given time. Cheng et al. [23] implemented a solar still using a shape-stabilized PCM; the experimental results revealed high thermal conductivity of about 1.50 W m K^{-1} with daily production of 3.41 L m^{-2} and overall efficiency of 21.5–57.5% for the solar still system. Xiaowei et al. [24] developed thin-film silicon solar cells using a Fourier-series-based periodic array. The results obtained for the optimized texture with thickness of 300 nm indicated a photocurrent of 27.05 mA cm^{-2} for silicon thickness of 1 µm, and angular analysis revealed that inverted pyramid and cosine surface arrays offered the best performance at all angles of incidence from about 0° to 65°.

Many researchers have investigated single-slope single-basin solar stills with the inclusion of water flowing over the glass cover, which has enormous application scope for the inclusion of drip technology, PCM, and nanoparticles in the system. Based on its operation, the internal heat transfer mode offers increased scope for advanced applications. The increased internal heat transfer in basin solar stills provides a new approach to increase production using this technology based on Nature.

Materials and methods

Investigation of water flowing over glass cover in a solar still with novel materials

Experimental analysis of a single-slope single-basin solar still with water flowing over the glass cover and novel (absorbing) materials (Fig. 1) was performed. The solar still comprised external and internal plywood mounts with an element size of 1.3 × 1.3 m and 1.25 × 1.25 m. The space between the attachments was filled with glass wool having thermal conductivity of 0.038 W m K^{-1}. The thickness of the back wall was 0.03 m, while that of the front wall was 0.10 m. A glass cover with thickness of 4 mm was applied as a secondary condensing surface with

Fig. 1 Experimental analysis of the effect of flowing water with novel fin materials

flowing water; the slope of the glass cover was fixed at 11°, near by equivalent to the latitude of its location (Chennai). It was made vaportight using metal putty. A J-shaped drainage channel was fixed to the front wall to accumulate the harvested water and the output slobbered miserable to the measuring jar. A classical experimental investigation of water flowing through the solar still was carried out as shown schematically in Fig. 2.

Heat transfer coefficient and productivity of still

The basin area of copper leaf and black paint was coated with Al_2O_3 nanoparticles in the inner area with novel absorbing wick materials to absorb surplus solar radiation. The solar radiation passing through the flowing water is transferred to the glass cover and novel fin wick materials (FWCM and FWJW) with Al_2O_3 to reach the copper coil and then the phase-change material ($C_{18}H_{36}O_2$). The absorption of solar radiation in the visible and IR parts of the spectrum is greatly intensified by the Al_2O_3 nanoparticles, enabling further heat transfer within the system. Saline water is passed sideways by pouring dropwise into

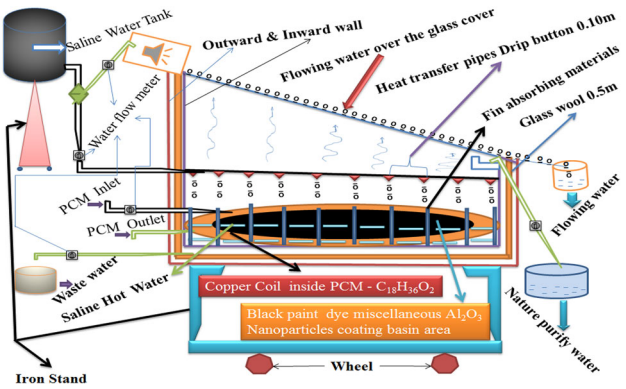

Fig. 2 Cross-sectional view of the solar still with flowing water and including novel materials

the absorbing material on the basin. The drip pipes for heat transfer coated with nanoparticles and black paint include drip buttons installed at intervals of 0.10 m, being separated horizontally in the basin in steps of 0.10 m.

The PCM material enables stable energy spreading by melting over a wide temperature range [25]. Various evaluations of such materials have been presented in literature [26–28] along with a full description of the latest progress on such materials and their thermophysical properties. Figure 3 summarizes this progress in the absorbing materials applied in the basin to improve the heat transfer, based on the cited reviews, using polymeric and solid–solid PCMs [29].

Figure 3 shows the new solar still that has been manufactured with a basin area including a fixed copper coil arrangement and immovable drip heat pipes. The configuration of the solar still is fixed with ten drip heat pipes and buttons separated at distances of 0.10 m × 0.10 m horizontally in the basin with south to north orientation. Exposed copper coil was fixed in the basin at intervals of 0.10 m with total length of 10 m.

The coil coated with black paint and Al_2O_3 nanoparticles increased the absorption of solar radiation and thus heat extraction, thereby improving the performance of the still using 8 kg of the PCM ($C_{18}H_{36}O_2$) inside the coiled basin area. Increasing the melting point of the PCM increases the evaporation from the solar still, as described in Refs. [30, 31]. The saline water tank is provided with a gate valve and is connected to the entrance of the dripping equipment.

Provisionally, the water flowing over the glass cover of the single-slope single-basin solar still was applied using a poly(vinyl chloride) pipe with quarter-inch diameter. The length of the pipe was taken precisely equal to the width of the still so that water would not flow lengthwise. Several holes were made in the pipe at equal spacings to maintain a uniform flow over the glass cover. The PVC pipe was clipped to the top of the glass cover. The water was collected at the lower end of the glass cover in a small plastic bucket. Due to the water flow over the glass cover, most of the heat was utilized for evaporation during the day, growth of midnight in this process. As expected, fast evaporation occurred due to the large temperature difference between the glass cover and water surface, as shown in Fig. 4, which shows the cooling effect of the water flowing over the experimental glass cover.

The temperature achieved when using the absorbing materials to condense the water flowing over the cover was measured using previously calibrated copper–constantan thermocouples. The intensity of solar radiation and the ambient temperature were measured using a solar radiation monitor and digital thermometer, respectively. Experiments were carried out on the solar still from 6 am to 6 am with duration of 24 h with water flowing over the glass cover using the absorbing materials during 2017 at the Research Center of Physics, Veltech Multitech Engineering College, Avadi, Chennai, 600 062 (latitude 13.1067°N, longitude 80.0970°E), Tamil Nadu, India.

Thermal modeling of solar still with novel absorbing materials

The solar radiation absorbed by the water flowing over the glass cover is transported over the absorbing materials as indicated by the internal heat transfer process shown in Figs. 1 and 4. The enhancement achieved by using PCM and nanoparticle fin wick absorbing materials when flowing water over the glass cover in the single-slope single-basin solar still was investigated by following the flowchart shown in Fig. 5. Figure 6 shows a schematic of the effect of water flowing over the glass cover on the surface of the absorbing materials on the production by the solar still, where the various labels indicate the parameters applied in the energy equilibrium equations. The analysis was based on the following assumptions:

1. The performance of the solar still (including PCM and nanoparticles) with water flowing over the glass cover based on the heat transfer ability of the surface of the

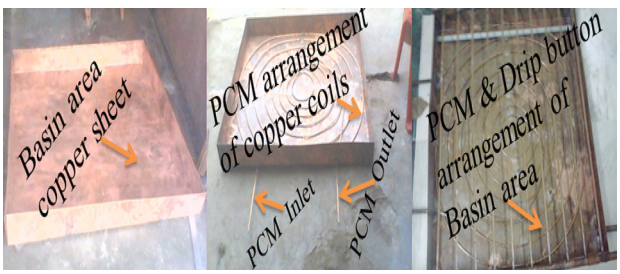

Fig. 3 Basin area arrangements with copper coil and fixed drip button heat pipes

Fig. 4 Experimental trials of water flowing over the glass cover of a solar still with novel absorbing materials

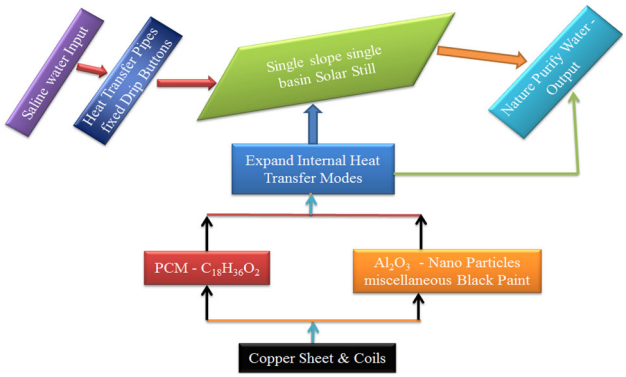

Fig. 5 Control flowchart of solar still

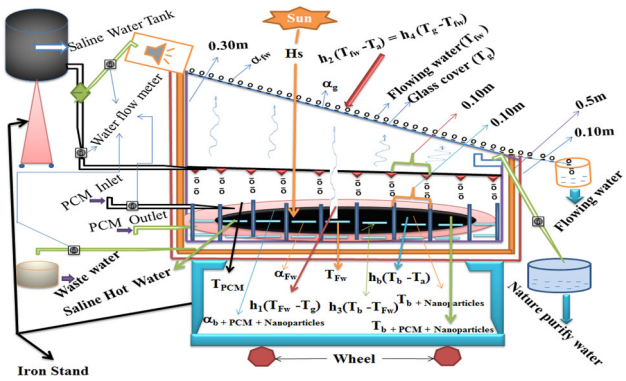

Fig. 6 Schematic of the solar still, including the parameters used in the action balance equations

absorbing materials was investigated assuming full insulation of the system and glass cover.

2. No heat escapes as vapor from the surface of the system.
3. The single-slope single-basin solar still with water flowing over the glass cover includes a surface made of absorbing materials and the distilled water component.
4. In the experimental work, the vapor pressure of water is assumed to be linear ($P = R_1T + R_2$) for the single-slope single-basin solar still.

Energy in the flowing water and its influence on the solar still

$$bl_{\mathrm{fw}}\rho c_{\mathrm{fw}}\frac{\mathrm{d}T_{\mathrm{fw}}}{\mathrm{d}t}\mathrm{d}x + m_{\mathrm{fw}}C_{\mathrm{fw}}\frac{\mathrm{d}T_{\mathrm{fw}}}{\mathrm{d}x}\mathrm{d}x = \alpha_{\mathrm{fw}}H_s b\mathrm{d}x + h_4(T_{\mathrm{g}} - T_{\mathrm{fw}})b\mathrm{d}x - h_2(T_{\mathrm{fw}} - T_{\mathrm{a}})b\mathrm{d}x. \tag{1}$$

Energy in the glass cover and absorbing materials and its influence on the solar still

$$H_s\alpha_{\mathrm{g}} + h_1\left(T_{\mathrm{Fw}} - T_{\mathrm{g}}\right) = h_4\left(T_{\mathrm{g}} - T_{\mathrm{fw}}\right). \tag{2}$$

Energy in the basin liner and absorbing materials of the solar still

$$\alpha_{(\mathrm{b+PCM+Nanoparticles})}H_s = h_3\left(T_{\mathrm{b+PCM+Nanoparticles}} - T_{\mathrm{Fw}}\right) + h_{\mathrm{b+PCM+Nanoparticles}}\left(T_{\mathrm{b+PCM+Nanoparticles}} - T_{\mathrm{a}}\right). \tag{3}$$

Energy in the water mass with absorbing materials of the solar still

$$\alpha_{\mathrm{Fw}}H_s + h_3\left(T_{\mathrm{b+PCM+Nanoparticles}} - T_{\mathrm{Fw}}\right) = M_{\mathrm{Fw}}C_{\mathrm{Fw}}\frac{\mathrm{d}T_{\mathrm{Fw}}}{\mathrm{d}t} + h_1\left(T_{\mathrm{Fw}} - T_{\mathrm{g}}\right), \tag{4}$$

where $h_1, h_2, h_3, h_4, h_{\mathrm{b+PCM+Nanoparticles}}$ are specified in the "Appendix."

Equation (1), after eliminating $T_{\mathrm{g}}\frac{\mathrm{d}T_{\mathrm{fw}}}{\mathrm{d}x} + a_1T_{\mathrm{fw}} = a_2T_{\mathrm{Fw}} + a_3$ from Eq. (2), can be reexpressed as

$$\frac{\mathrm{d}T_{\mathrm{fw}}}{\mathrm{d}x} + a_1T_{\mathrm{fw}} = a_2T_{\mathrm{Fw}} + a_3, \tag{5}$$

where

$$a_1 = \frac{(h_4 + h_2)b}{m_{\mathrm{fw}C_{\mathrm{fw}}}} + \frac{h_4^2 b}{(h_4 + h_2)m_{\mathrm{fw}C_{\mathrm{fw}}}},$$

$$a_2 = \frac{(h_1h_4)b}{(h_4 + h_2)m_{\mathrm{fw}C_{\mathrm{fw}}}},$$

$$a_3 = \frac{\alpha_{\mathrm{fw}}H_s b}{m_{\mathrm{fw}C_{\mathrm{fw}}}} + \frac{\alpha_{\mathrm{g}}H_s h_4 b}{(h_4 + h_1)m_{\mathrm{fw}C_{\mathrm{fw}}}} + \frac{(h_4 + h_2)b}{m_{\mathrm{fw}C_{\mathrm{fw}}}}.$$

Equation (5) can be rewritten as

$$T_{\mathrm{fw}} = \frac{(a_2T_{\mathrm{Fw}} + a_3)}{a_1} + C\mathrm{e}^{-a_1t}. \tag{6}$$

Equation (6) is subject to the following initial conditions for the still:

$$T_{\mathrm{fw}} = T_{\mathrm{fw0}} \quad \text{For all value of } t \text{ at } x = 0 \tag{7}$$

Substitution of the equation for c into Eq. (6) yields

$$T_{\mathrm{fw}} = \frac{(a_2T_{\mathrm{Fw}} + a_3)}{a_1}[1 - \mathrm{e}^{-a_1t}] + T_{\mathrm{a}}\mathrm{e}^{-a_1t}. \tag{8}$$

Equation (8) is the required explicit expressions for the temperatures of the flowing water and glass cover of the still, respectively.

The variations of the solar radiation and ambient temperature are periodic and can be expressed in Fourier series in the following form according to Torchia-Nunezl et al. [32]:

$$f(t) = a_0 + \sum_{n=1}^{\infty}(A_n \cos n\omega t + B_n \sin n\omega t). \tag{9}$$

The variation of the hydraulic flow over a glass screen with a fin wick material in a solar still was expressed by Rahoma and Hassan [33] as

$$f(t) = a_0 + \sum_{n=1}^{\infty} A_n \exp(in\omega t).$$

Since the solar radiation and ambient temperature are periodic in nature, they can be subject to Fourier analysis for the solar still, as follows:

$$H_s(t) = H_0 + \sum_{n=1}^{\infty} H_{sn} \exp(in\omega t), \tag{10}$$

$$T_a(t) = T_{a0} + \sum_{n=1}^{\infty} T_{an} \exp(in\omega t), \tag{11}$$

$$T_g(t) = T_{g0} + \sum_{n=1}^{\infty} T_{gn} \exp(in\omega t), \tag{12}$$

$$T_{fw}(t) = T_{fw0} + \sum_{n=1}^{\infty} T_{fwn} \exp(in\omega t), \tag{13}$$

and

$$T_{Fw}(t) = T_{Fw0} + \sum_{n=1}^{\infty} T_{Fwn} \exp(in\omega t), \tag{14}$$

where the constants $T_{g0}, T_{fw0}, T_{Fw0}, T_{gn}, T_{fwn}, T_{Fwn}$ are determined by substituting for

$$H_s(t), T_a(t), T_g(t), T_{fw}(t) \text{ and } T_{Fw}(t)$$

with the help of Eqs. (10–14) in Eqs. (2), (8), and (4) with integration using the initial condition $T_{Fw} = T_{Fw0}$ at $t = 0$ as

$$T_{Fw}(t) = \frac{b_0}{a_4}(1 - e^{-a_4 t}) + T_{Fw0}e^{-a_4 t} + \sum_{n=1}^{\infty} \frac{b_n}{i\omega n + a_4}(e^{in\omega t} - e^{-a_4 t}), \tag{15}$$

where b_0 is the time-independent component of $b(t)$; b_0 is the coefficient of the time-dependent component of $b(t)$, taking the form

$$b_0 = a_5 H_{s0} + a_6 T_{a0},$$

$$b_n = a_5 H_{sn} + a_6 T_{an},$$

where

$$a_4 = \frac{h_1 + h_2}{m_{Fw} C_{Fw}} - \frac{h_3^2}{(h_3 + h_{b+PCM+Nanoparticles}) m_{Fw} C_{Fw}} - \frac{h_1^2 h_1 h_4}{(h_4 + h_1) m_{Fw} C_{Fw}} \left(\frac{a_2}{a_1}\right)(1 - e^{-a_1 t}),$$

$$a_5 = \frac{\alpha_{Fw}}{m_{Fw} C_{Fw}} + \frac{h_3 \alpha_g}{(h_3 + h_{b+PCM+Nanoparticles}) m_{Fw} C_{Fw}} + \left(\frac{h_1 \alpha_g}{(h_4 + h_1) m_{Fw} C_{Fw}}\right)\left(\frac{b \alpha_{fw}}{a_1 m_{fw} C_{fw}}\right)(1 - e^{-a_1 t}),$$

$$a_6 = \frac{h_3 h_{b+PCM+Nanoparticles}}{(h_3 + h_{b+PCM+Nanoparticles})} + \frac{h_4 h_1}{h_4 + h_1} e^{-a_1 t} + \frac{h_1 h_4}{(h_4 + h_1)} \left(\frac{h_2 b}{m_{fw} C_{fw}}\right)\left(\frac{a_3}{a_1}\right)(1 - e^{-a_1 t}).$$

The values of $T_{Fw}(t)$ are designed at intervals of 1/2 h starting from sunrise according to Eq. (15), and $T_g(t)$ is calculated from the relation

$$T_{gn} = \frac{H_s \alpha_g + h_1 T_{Fwn} + h_4 T_{fw}}{h_4 + h_1}. \tag{16}$$

During off-sunshine hours, the solar intensity and integration limit will dissipate, then the analysis will be the same.

The instantaneous effect on the distillate production of each novel material is expressed as

$$m_e = \frac{h_{ewg}(T_{Fw}(t) - T_g(t))}{L} \times 3600. \tag{17}$$

The efficiency of the proposed structure can be expressed as

$$\eta\% = \frac{M_e L}{A_{b+PCM+Nanoparticles} \int Hs \Delta t} \times 100, \tag{18}$$

where Δt refers to the time interval over which the solar intensity is measured.

Results and discussion

Numerical calculations were carried out to investigate the effect of the fin with cotton wick (FWCW) and fin with jute wick (FWJW) on the basin surface area. Hourly data for the solar intensity (PCE-SPM 1 detector, IEC 61724-1 and ISO 9060 pyranometers), signal range (SR01 pyranometers), and ambient temperature monitored on two typical summer days in 2017 at Chennai are presented in Table 1. The Fourier coefficients of the solar intensity and ambient temperature were evaluated using Fourier series with harmonics from 6 to −6.

The instantaneous thermal efficiency of the proposed solar still with water flowing over the glass cover including FWCW and FWJW was evaluated using the following parameter values:

Table 1 Solar radiation measurement summary

S. no	Instrument	Range	Accuracy (%)
1	RTD sensors (PT100)	−267 to 260 °C	±0.1 °C
2	Signal range (SR01 pyranometers)	0–2000 W m^{-2}	±0.05 W m^{-2}
3	Collecting jar	0–1000 mL	±10 mL
4	Anemometer	0–50 m s^{-1}	±0.2 m s^{-1}

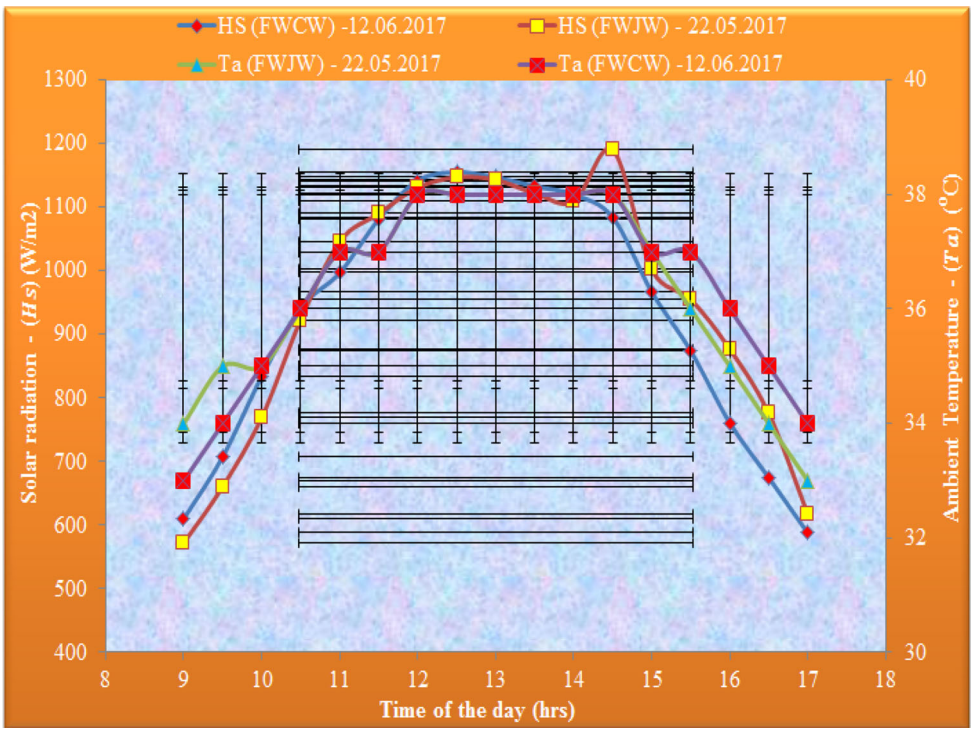

Fig. 7 Hourly variation of solar radiation absorption and ambient temperature for the solar still

$A_g = 1.69\ m^2$, $\tau_g = 0.75$, $A_w = 1.69\ m^2$, $M_w = M_{fw} = 12$ kg, $\varepsilon_g = 0.88$, $\sigma = 5.66 \times 10^{-8}$ W m^{-2} K^{-4}, $\alpha_g = 0.05$, $C_w = 4190$ J kg^{-1}, $V = 1.4$ m $K^{-1} = 0.038$ W m K^{-1}, $h_1 = 22.52$ W m^{-2} °C^{-1}; $h_2 = 15.64$ W m^{-2} °C^{-1}; $h_3 = 137.05$ W m^{-2} °C^{-1}; $h_4 = 135.5$ W m^{-2} °C^{-1}; $h_b = 0.7686$ W m^{-2} °C^{-1}; $h_{ew} = 14.01$ W m^{-2} °C^{-1}; $h_i = 6.27$ W m^{-2} °C^{-1}; $K_i = 0.04$ W m^{-2} °C^{-1}; $L = 2372.52$ kJ kg^{-1}; $l_i = 0.05$ m; $\omega = 7.2722 \times 10^{-5}$ s^{-1}; $\tau_w = 0.1$; $\tau_{fw} = 0.0$; $\tau_b = 0.6$; $\alpha_{fw} = \alpha_w = \alpha_b = 0.88$; $\rho = 1000.0$ kg m^{-3}; $C_w = C_{fw} = 4190$ J kg^{-1} °C^{-1}.

The solar still was implemented for high thermal energy accumulation based on the benefits provided by the PCM and nanoparticles for absorption of solar intensity at ambient temperature for 2 days with the absorbing wick materials, i.e., FWCW and FWJW; the results obtained on typical summer days are shown in Fig. 7. The absorbing materials were evaluated using the Fourier coefficients H_s and T_a for 2017 at Chennai, Tamil Nadu, India.

It is clear that the 6 to −6 harmonics used in the analysis are adequate to achieve convergence of the Fourier series in Tables 2 and 3. The hourly variation of the solar still showed the same trend on all days, and the solar radiation appeared to be maximum from 12 to 2 pm.

The numerical and experimental results obtained for the proposed solar still with and without PCM and nanoparticles in the basin liner in terms of the increase in the temperatures of the FWCW/FWJW, glass cover, and flowing water are shown in Figs. 8a and 9.

It is clear that the results for the temperatures of the FWCW and FWJW obtained experimentally and theoretically showed the same tendency. This innovative solar still manufactured based on internal heat transfer modes with numerous enhancements including the stable PCM basin liner reached a temperature of only 35 °C, while for that using the PCM and nanoparticles, the temperature peaked at 70 °C (copper coils) and the black paint with

Table 2 Fourier coefficients of H_s from 6 to −6 harmonics, confirming convergence of the Fourier series

n	Real	Imaginary
Fourier coefficient of H_s		
0	262.107	
6	1.015	2.441
5	2.008	− 2.103
4	− 8.001	− 8.018
3	− 31.055	− 31.055
2	114.053	− 61.667
1	− 78.096	− 27.360
−1	177.075	− 1.091
−2	145.073	− 82.950
−3	52.032	− 52.253
−4	25.268	− 17.123
−5	12.246	− 6.324
−6	4.171	− 5.232

Table 3 Fourier coefficients of T_a from 6 to −6 harmonics, confirming convergence of the Fourier series

n	Real	Imaginary
Fourier coefficients of T_a		
0	38.305	
6	0.284	0.564
5	6.587	− 0.290
4	− 0.976	− 0.612
3	−1.654	− 0.543
2	4.432	− 2.387
1	− 2.960	− 10.365
−1	0.675	− 2.853
−2	0.523	− 2.654
−3	0.198	− 0.189
−4	0.105	− 0.743
−5	0.994	− 0.664
−6	0.321	− 0.754

nanoparticles (basin) temperature increased the solar radiation absorbed by the system, resulting in the hourly temperature variation shown in Fig. 8b. The properties of the PCM and nanoparticles used in the basin liner are presented in Table 4.

The hourly variation of the production rate, FWCW and FWJW temperatures, glass cover temperature, and flowing water temperature when using the basin liner with PCM and nanoparticle absorbing materials and dripping pure saline water to maintain the minimum water depth is compared in Fig. 10.

From this figure, it is clear that, when using PCM and nanoparticles with saline water in the absorbing materials, the rate of evaporation was increased due to the large temperature difference between the absorbing materials and glass cover. The variation of the temperature among the absorbing materials and glass cover without PCM and nanoparticles is small due to their huge thermal ability, while the amount of evaporation is moderate. The maximum distillate harvest obtained with the structure including the FWCW and FWJW was 0.469 and 0.415 kg m^{-2} in 30 min during the period from 12.30 to 14:00, compared with 0.250 and 0.244 kg m^{-2} in 30 min without PCM and nanoparticles. The total distillate harvest with the FWCW and FWJW from 9 am to 17 pm was found to 6.699 kg m^{-2} and 5.659 kg m^{-2}, compared with 3.343 kg m^{-2} and 3.014 kg m^{-2} without PCM and nanoparticles. Hence, the peak illumination of the solar still with the PCM and nanoparticles and the FWCW and FWJW resulted in the distillate harvest, as well as a nocturnal output of 2.730 kg m^{-2} and 2.130 kg m^{-2}. Over the

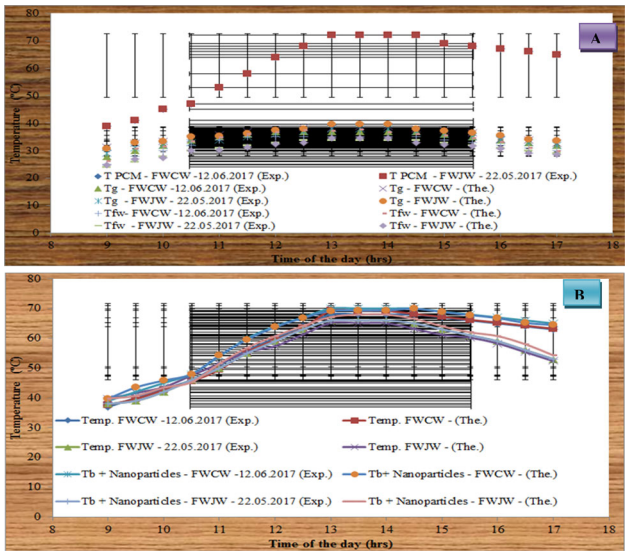

Fig. 8 (A, B) Effect of PCM and nanoparticles on hourly variation of temperatures of FWCW, FWJW, glass cover, flowing water, and basin (nanoparticles) of solar still

24-h cycle, the overall production of the proposed system with the FWCW and FWJW was found to be 9.429 kg m^{-2} day^{-1} and 7.789 kg m^{-2} day^{-1}, compared with the values of 5.234 kg m^{-2} day^{-1} and 4.434 kg m^{-2} day^{-1} without PCM and nanoparticles. The numerical results for the temperatures of the FWCW, FWJW, glass cover, flowing water, and basin liner agreed well with the experimental observations. The instantaneous efficiency of the absorbing materials in the proposed structure was established and is shown in Fig. 11. The

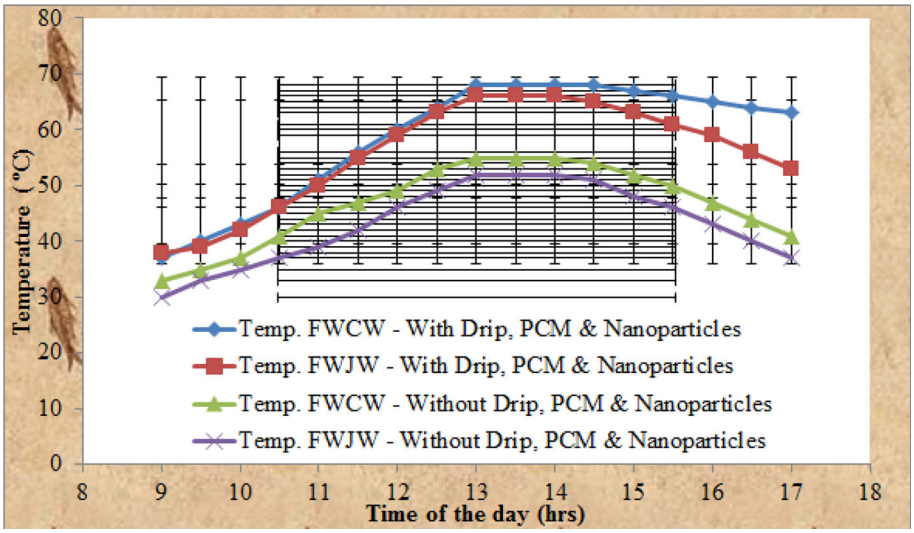

Fig. 9 Hourly variation of absorbing materials, comparing the solar still systems with and without dripping, PCM, and nanoparticles

Table 4 Materials properties of the Al_2O_3 nanoparticles and PCM

S. no.	Nanoparticles	Concentration/size of particles/%	Specific surface area/m^2 g^{-1}	Density/ kg m^{-3}	Thermal conductivity/ W m^{-1} K^{-1}	Enhancement/%
1	Al_2O_3	50 nm	1 × 1	3890	30	99.99
	Compound	Melting temperature (°C)	Heat of fusion (kJ kg^{-1})	Density (kg m^{-3})	Thermal conductivity (W m^{-1} K^{-1})	Application (%)
2	Stearic acid	72	208	853	0.178	Solar still (FWCW) 70.02

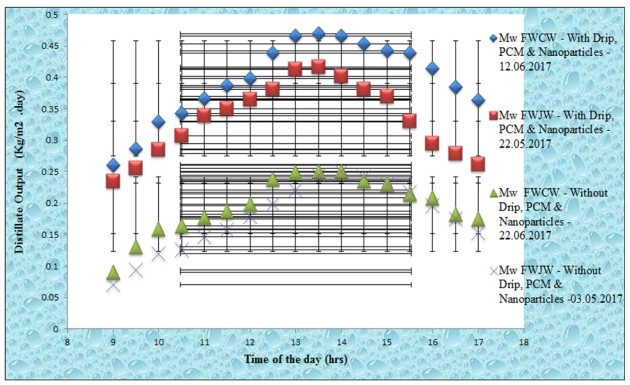

Fig. 10 Hourly variation of distillate production with and without novel PCM and nanoparticle materials

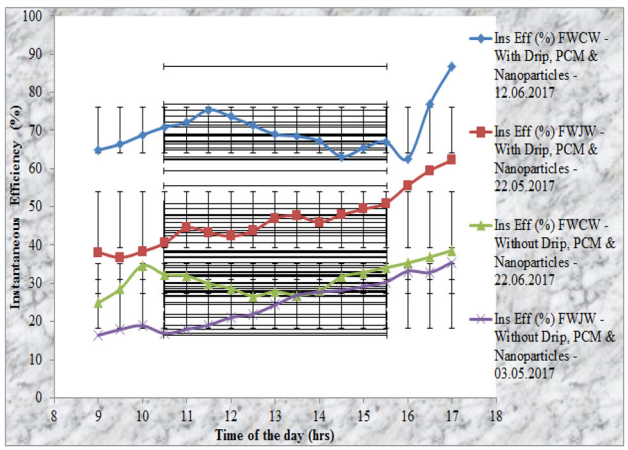

Fig. 11 Hourly variation of instantaneous energy efficiency of the solar still with absorbing materials with and without PCM and nanoparticles

absorptivity of the wick surface is an important operational parameter of the solar still and should be chosen optimally to enhance the efficiency. The water flowing over the glass cover influenced the instantaneous overall efficiency of the systems with FWCW and FWJW with and without PCM and nanoparticles from 70.02% to 46.69% and 31.19% to 24.62%, respectively. These results indicate that the instantaneous distillate harvest with PCM and nanoparticles and water flowing over the glass cover in the solar still

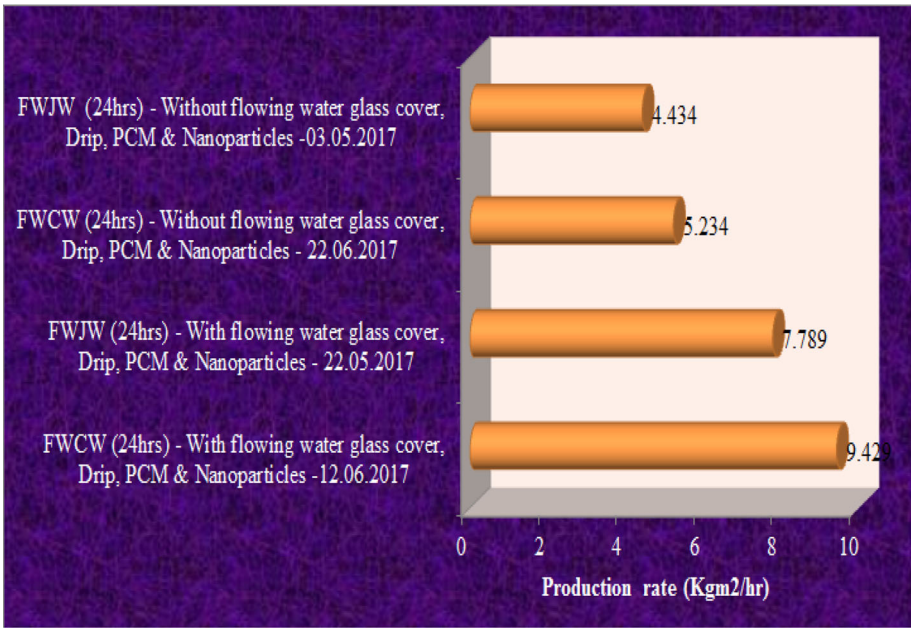

Fig. 12 Effect of absorbing materials on the energy absorption by the solar still over 24 h and its production with and without PCM and nanoparticles

Table 5 Comparison of a muse and manifold duty concerning solar still with have flowing water over the glass, drip, nanoparticles, and PCM

S. no	Ref.	Modification	Productivity/%
1	Sharshir et al. [22]	A: FGN	50.28
		B: PCM and FG	65.00
		C: FGN and film cooling	56.15
		D: FGN, PCM, and film cooling	73.80
2	Nijmeh et al. [36]	$KMnO_4$	26
		$K_2Cr_2O_7$	17
3	Elango et al. [37]	Al_2O_3	29.95
		Fe_2O_3	18.63
		ZnO	12.67
4	Sahota and Tiwari [19]	Al_2O_3	12.2
5	Kabeel et al. [38]	Al_2O_3	11.6
6	Shakthivel et al. [19]	Regenerative effect and jute cloth	20
7	Dhiman and Tiwari [40]	Water flow over glass cover and multiwick	10
8	Present work	Flowing water over the glass cover, drip, PCM, and Al_2O_3	70.02

was 25% higher than that without PCM and nanoparticles. Furthermore, the theoretical results confirm that the experimental explanations are good, showing no discrepancy in their tendency.

The numerical results for the temperatures of the FWCW, FWJW, glass cover, flowing water, and basin liner of the solar still showed close agreement with the observed energy in the form of heat, leading to higher efficiency and an increase in the saturated vapor pressure, as confirmed by Huang et al. and Shanmugan et al. [34, 35]. This enhancement is achieved by the nanoparticles, which are found to be hydrophobic, with the assistance of the PCM to achieve fast evaporation and thereby more vapor for enhanced water production.

Figure 12 compares the total productivity over 24 h with flowing water over the glass for the solar still with FWCM in the basin with and without PCM and nanoparticles, showing a value of 9.429 kg m^{-2} day^{-1}. Table 5 compares the present research with various other works on solar stills with flowing water over the glass, dripping,

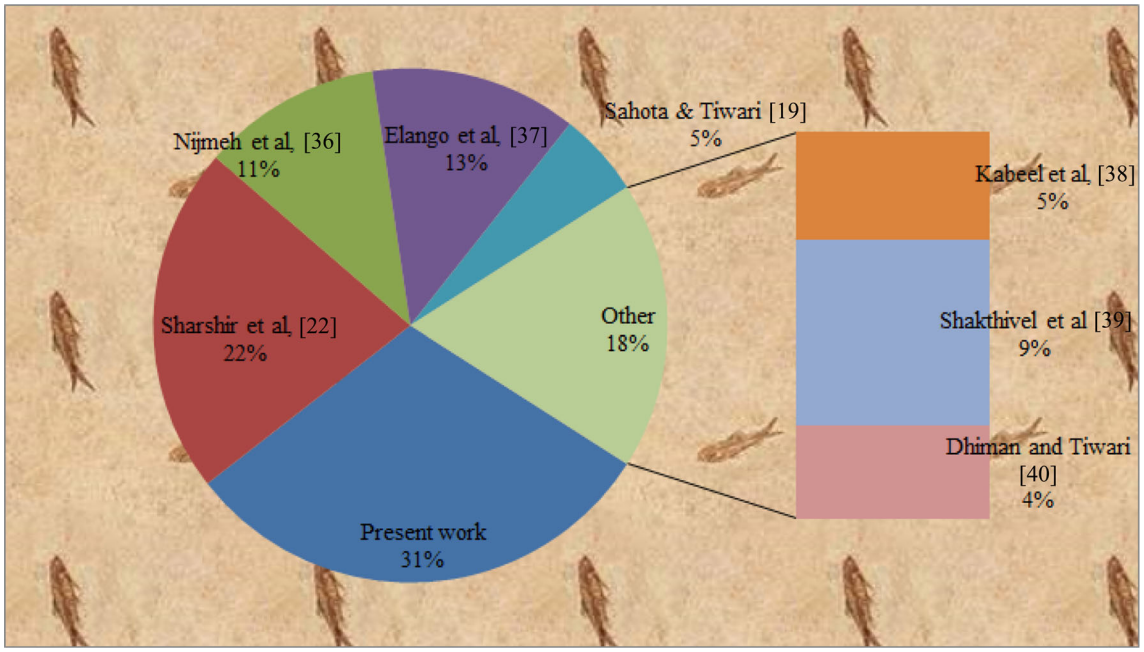

Fig. 13 Comparison of overall effectiveness of solar still with water flowing over the glass, drip, PCM, and nanoparticles

Table 6 Water analysis before and after processing by the solar still

Desalination			Standards
Parameter	Before	After	World Health Organization
pH	9.1	6.1	6.5–8.5
Electrical conductivity (μS cm^{-1})	5.20	0.31	< 250
Total dissolved solids (mg L^{-1})	185.4	89.6	< 600
Redox (mV)	196.1	164.8	–
Salinity (ppm)	148.3	71.7	< 250
Arsenic (ppm)	0.3	0.001	0.01
Coliform bacteria (*N* 100 mL^{-1})	0	0	0

Water before and after desalination checked by the laboratory of the National Agro Foundation (NAF)

nanoparticles, and PCM. Figure 13 compares the overall maximum efficiency results for the solar still with water flowing over the glass, drip, PCM, and nanoparticles.

Analysis of water quality before and after solar still

A new solar still is proposed for natural purification of standard water (H_2O) and removal of contaminants. The water parameters achieved by the overall experimental work are presented in Tables 6 and 7. The aim of this process is to elevate the pH, electrical conductivity (EC),

Table 7 Cost analysis of solar still

S. no.	Material	Price (Rs)
1	Copper sheet and coils, 4 mm × 5 kg	25,000
2	Glass	750
3	Insulation and sealing (silicone glue)	2850 + 650 = 3500
4	Plywood (outer and inner walls)	1500
5	Carbon black paint	100
6	PCM, $C_{18}H_{36}O_2$	1200
7	Al_2O_3 nanoparticles	3500
8	FWCW and FWJW	2500
9	Hoisting mechanism and other auxiliary equipment	1000
10	Labor and machining	3500
11	Temperature sensor	1555
12	Other parts (piping and tank)	1000
13	Report writing (typing, editing, color printing, binding)	1500
14	Al pipe	250
15	Water testing	1200
16	Net cost of project	48,055

total dissolved solids (TDS), and total hardness through the solar desalination process. The distilled water produced by the solar still was subjected to drinking water control and verification by the laboratory of the National Agro Foundation (NAF), Tharamani, Chennai, Tamil Nadu, 600113 India.

Conclusions

The relationships affecting the instantaneous productivity of a still for use in solar thermal applications were investigated and confirmed, and the effect of the dripping, PCM, and nanoparticles investigated, with the following results:

1. The water flowing over the glass cover shows an absorption effect, with good agreement between the theoretical and experimental results for the structure.
2. The operation of the system was enhanced by the inclusion of PCM and nanoparticles due to their effect on the thermal transfer, storage density, and isothermal nature of the solar still.
3. The daily distillate production rate of the still was enhanced by the application of drip buttons for pure saline water, increasing the absorptive effect of the FWCW by 70.02%. When using the FWCW, the surface should be lifted up to eliminate salt deposition.
4. The superior production of the solar still with the FWCW reached 9.429 kg m^{-2} day^{-1}, with the water flowing over the glass cover having an effect of 13.37%, being 25% higher than the result without PCM and nanoparticles.
5. The absorbing materials and water flowing over the glass cover with the PCM and nanoparticles enhanced the performance of the solar still in terms of the solar intensity and ambient temperature, as confirmed by the good agreement between the Fourier analysis using 6 to –6 harmonics and the observations.

Appendix

The experimental work on the solar still with water flowing over the glass cover with absorbing materials was carried out out from 6 am to 6 am (24 h duration), as well as measurements of the evaporative, convective, and radiative heat transfer coefficient during 2017 at the Research Center of Physics, Veltech Multitech Engineering college, Avadi, Chennai, 600 062 [latitude 13.1067°N, longitude 80.0970°E], Tamil Nadu, India, where the atmosphere can be expressed as follows:

$$h_4 = 0.016 \times h_2 \times (P_{\mathrm{fw}} - \gamma P_{\mathrm{a}}), \tag{19}$$

$$P_{\mathrm{fw}} = R_1 T_{\mathrm{fw}} + R_2,$$

$$\gamma P_{\mathrm{a}} = R_1 T_{\mathrm{a}} + R_2,$$

$$h_1 = h_{\mathrm{cwg}} + h_{\mathrm{ewg}} + h_{\mathrm{rwg}}, \tag{20}$$

$$h_{\mathrm{cwg}} = 0.884 \times \left[\left(T_{\mathrm{Fw}} - T_{\mathrm{g}}\right) + \frac{\left(P_{\mathrm{Fw}} - P_{\mathrm{g}}\right)\left(T_{\mathrm{Fw}} + 273\right)}{268,900 - P_{\mathrm{Fw}}} \right]^{1/3},$$

$$h_{ewg} = 0.016273 \times h_{cwg}\left(\frac{P_{Fw} - P_g}{T_{Fw} - T_g}\right),$$

$$h_{rwg} = \frac{\varepsilon\sigma\left[(T_{Fw}+273)^4 - (T_g+273)^4\right]}{(T_{Fw} - T_g)},$$

$$h_2 = h_{cwa} + h_{rwa}, \tag{21}$$

$$h_{ca} = 5.7 + 3.8\,V,$$

$$h_{cwa} = 0.884 \times \left[(T_{Fw} - T_a) + \frac{(P_{Fw} - P_a)(T_{Fw}+273)}{268,900 - P_{Fw}}\right]^{1/3},$$

$$h_{rwa} = \frac{\varepsilon\sigma\left[(T_{Fw}+273)^4 - (T_a+273)^4\right]}{(T_{Fw} - T_a)},$$

$$m_{fw} = bl_w,$$

where l_w is the thickness of flowing water over the glass cover

$$h_3 = h_{cbw} + h_{rbw}, \tag{22}$$

$$h_{cbw} = 0.884 \times \left[(T_{b+PCM+Nanoparticles} - T_w) + \frac{(P_{b+PCM+Nanoparticles} - P_w)(T_{b+PCM+Nanoparticles}+273)}{268,900 - P_b}\right]^{1/3},$$

$$h_{rbw} = \frac{\varepsilon\sigma\left[(T_{b+PCM+Nanoparticles}+273)^4 - (T_w+273)^4\right]}{(T_{b+PCM+Nanoparticles} - T_w)},$$

$$h_4 = h_{cgw} + h_{rgw}, \tag{23}$$

$$h_{cgw} = 0.884 \times \left[(T_g - T_w) + \frac{(P_g - P_w)(T_g+273)}{268,900 - P_g}\right]^{1/3},$$

$$h_{rgw} = \frac{\varepsilon\sigma\left[(T_g+273)^4 - (T_w+273)^4\right]}{(T_g - T_w)},$$

$$h_3 = h_{cbw} + h_{rbw}, \tag{24}$$

$$h_{cbw} = 0.884 \times \left[(T_{b+PCM+Nanoparticles} - T_w) + \frac{(P_{b+PCM+Nanoparticles} - P_w)(T_{b+PCM+Nanoparticles}+273)}{268,900 - P_{b+PCM+Nanoparticles}}\right]^{1/3},$$

$$h_{rbw} = \frac{\varepsilon\sigma\left[(T_{b+PCM+Nanoparticles}+273)^4 - (T_w+273)^4\right]}{(T_{b+PCM+Nanoparticles} - T_w)},$$

where the temperature of the flowing water at $x = 0$ and glass cover is the instantaneous glass temperature for each hour.

References

1. Prakash J, Kavatherkar AK. Performance prediction of a regenerative solar still. Solar Wind Technol. 1986;3(2):119–25.
2. Singh AK, Tiwari GN. Experimental validation of passive regenerative solar still. Int J Energy Res. 1992;16(6):497–506.
3. Singh AK, Tiwari GN. Design parameters of an active regenerative solar still: an experimental study. Int J Energy Res. 1993;17(5):365–75.
4. Sanjaykumar SS. Transient model and comparative study of concentrator coupled regenerative solar still in forced circulation mode. Energy Convers Manag. 1996;37(5):629–36.
5. Prasad B, Bhagat N, Tiwari GN. Enhancement in daily yield due to regenerative effect in solar distillation. Int J Ambient Energy. 1997;18(2):83–92.
6. Sangeeta S, Tiwari GN. Effect of water flow on internal heat transfer solar distillation. Energy Convers Manag. 1999;40:509–18.
7. Zurigat YH, Abu-Arabi MK. Modeling and performance analysis of a solar desalination unit with double-glass cover cooling. Desalination. 2001;138:145–59.
8. Zurigat YH, Abu-Arabi MK. Modeling and performance analysis of a regenerative solar desalination unit. Appl Therm Eng. 2004;24(7):1061–72.
9. Janarthanan B, Chandrasekaran J, Kumar S. Performance of floating cum-tilted wick type solar still with the effect of water flowing over the glass cover. Desalination. 2006;190:51–62.
10. Murugavel KK, Chockalingam KSK, Srithar K. Progresses in improving the effectiveness of the single basin passive solar still. Desalination. 2008;220(1–3):677–80.
11. Boutebila H. A theoretical model of a free flow solution over an inclined long flat plate solar still. Desalination. 2009;249:1249–58.
12. Zeroual M, Bouguettaia H, Bechki D, Boughali B, Bouchekima S, Mahcene H. Experimental investigation on a double slope solar still with the partially cooled condenser in the region of Ouargla (Algeria). Energy Procedia. 2011;6:736–42.
13. Dea Sabah R, Abdul-wahab A, Tiwari GN. Performance study of the inverted absorber solar still with water depth and total dissolved solid. Appl Energy. 2011;88:252–64.
14. Abdul Jabber KN. On the effect of the cover tilt angle of the simple solar still on its productivity in different seasons and latitudes. Energy Convers Manag. 2011;52:431–6.
15. Sandeep Kumar S, Dwivedi VK. Experimental study on the modified single slope single basin active solar still. Desalination. 2015;367:69–75.
16. Shanmugan S, Manikandan V, Shanmugasundaram K, Janarathanan B, Chandrasekaran J. Energy and exergy analysis of single slope single basin solar still. Int J Ambient Energy. 2012;33:142–51.
17. Rahmani A, Boutria A, Hadef A. An experimental approach to improve the basin type solar still uses an integrated natural circulation loop. Energy Convers Manag. 2015;93:298–308.
18. Ayman GM, Ibrahim S, Elshamarka E. Performance study of a modified basin type solar still. Sol Energy. 2015;118:397–409.
19. Sahota L, Tiwari GN. Effect of Al_2O_3 nanoparticles on the performance of passive double slope solar still. Sol Energy. 2016;130:260–72.

20. Shanmugan S, KottaiRaj M, Ragh S, Arunnarayanan M. Design and performance analysis of an innovative V-shape double slope tribasin solar nano still. Int J Appl Eng Res. 2015;10(83):261–6.
21. Sellamia MH, Belkisa Aliouara ML, Meddoura SD, Bouguettaiab H, Loudiyic K. Improvement of solar still performance by covering absorber with blackened layers of sponge. Groundw Sustain Dev. 2017;5:111–7.
22. Sharshir SW, Peng G, Wn L, Essa FA, Kabeel AE, Yang N. The effects of flake graphite nanoparticles PCM and film cooling on the solar still performance. Appl Energy. 2017;191:358–66.
23. Cheng WL, KaiHuo Y, LeNian Y. Performance of solar still using shape-stabilized PCM: experimental and theoretical investigation. Desalination. 2019;455:89–99.
24. Guo X, Wang D, Wenlong XU, Li S, Tanga P. Adsorption enhancement in thin-film silicon solar cells with a Fourier-series based periodic array. Opt Mater Express. 2017;7(3):793–8.
25. Zhou D, Zhao C, Tian Y. Review on thermal energy storage with phase change materials (PCMs) in building applications. Appl Energy. 2012;92:593–605.
26. Pielichowska K, Pielichowski K. Phase change materials for thermal energy storage. Prog Mater Sci. 2014;65:67–123.
27. Shalabyet SM. An experimental investigation of a V-corrugated absorber single-basin solar still using PCM. Desalination. 2016;398:247–55.
28. Sakthivel TG, Arjunan TV. Thermodynamic performance comparison of single slope solar stills with and without cotton cloth energy storage medium. J Therm Anal Calorim. 2018. https://doi.org/10.1007/s10973-018-7909-0.
29. Wu B, Zhao Y, Liu Q, Zhou C, Zhang X, Lei J. Form-stable phase change materials based on castor oil and palmitic acid for renewable thermal energy storage. J Therm Anal Calorim. 2019. https://doi.org/10.1007/s10973-019-08041-x.
30. Harahsheha MA, Arabiab MA, Mousaac H, Zghoula ZA. Solar desalination using solar still enhanced by external solar collector and PCM. Appl Therm Eng. 2018;128:1030–40.
31. Madalina GM, Minea AA, Huminic G, Huminic A. Al_2O_3/TiO_2 hybrid nanofluids thermal conductivity an experimental approach. J Therm Anal Calorim. 2018. https://doi.org/10.1007/s10973-018-7974-4.
32. Torchia-Nunezl JC, Cervantes-de-Gortari J, Porta-Gandara MA. Thermodynamics of a shallow solar still. Energy Power Eng. 2014;6:246–65.
33. Ali Rahoma U, Hassan AH. Fourier transforms investigation of global solar radiation at true noon: in the desert climatology. Am J Appl Sci. 2007;4(11):902–7.
34. Huang Z, Li X, Yuan H, Feng Y, Zhang X. Hydrophobically modified nanoparticle suspensions to enhance water evaporation rate. Appl Phys Lett. 2016;109:161–702.
35. Shanmugan S, Palani S, Janarthanan B. Productivity enhancement of solar still by PCM and nanoparticles miscellaneous basin absorbing materials. Desalination. 2018;433:186–98.
36. Nijmeh S, Odeh S, Akash B. Experimental and theoretical study of a single-basin solar still in Jordan. Int Commun Heat Mass Transfer. 2005;32:565–72.
37. Elango T, Kannan A, Murugavel KK. Performance study on single basin single slope solar still with different water nanofluids. Desalination. 2015;360:45–51.
38. Kabeel AE, Omara ZM, Essa FA. Enhancement of modified solar still integrated with external condenser using nanofluids: an experimental approach. Energy Covers Manag. 2014;78:493–508.
39. Sakthivel S, Sundaram S, Alwarsamy T. An experimental study on a regenerative solar still with energy storage medium-jute cloth. Desalination. 2010;264(1–2):24–31.
40. Dhiman NK, Tiwari GN. Effect of water flowing over the glass cover of a multi-wick solar still. Energy Convers Manag. 1990;30(3):245–50.